Establishment of mouse Embryonic Stem cell lines with a reporter of *Dll1* activity

Rúben Duarte Magalhães Alves Pereira

Mestrado Integrado em Engenharia Biomédica
Instituto Superior Técnico
Lisboa, Portugal

rubens.dmap@gmail.com

Abstract

The work described here aims to contribute to the understanding of Notch pathway, particularly to enlighten the possible correlation between *Notch* and the cell cycle during neurogenesis. Specifically, this work aims to generate a transgenic mouse ES cell lines containing a fluorescent reporter for the purpose of visualizing the activity of *Dll1* in ES cells using BAC recombineering. Therefore, the work performed was divided in two important parts for this project.

The first part of the work aimed to contribute to the generation of the transgenic mouse ES cells line, namely by establishing a reproducible and consistent BAC extraction, as well as a visualization protocol. This objective was achieved by studying the several steps of DNA extraction using a commercial kit and a "traditional extraction" protocol that were compared a posteriori. This study revealed several weaknesses of the commercial kit and led to the establishment of an extraction protocol based on one described by Bill Richardson and Nicoletta Kessaris, in 2006.

In the second part, the aim was to contribute to the validation of the model used in the lab, namely concerning the relation between *Dll1* expression, INM and cell cycle in the rosettes. For this, we did immunocytochemistry assays in mouse ES cells with a fluorescent reporter for *Dll1* activity, amplified and differentiated *in vitro*, and concluded that their behavior might be considered analogous to that observed in cells from the neural tube (*in vivo*).

Key-words: BAC extraction, PFGE, *Delta-like1* (*Dll1*), fluorescent reporter, ES cells.

Introduction

The Notch signaling pathway is important for cell-cell communication, and involves gene regulation mechanisms that control multiple cell differentiation processes during embryonic and adult life. It was also shown to be deregulated in many cancers and disease states.

The vertebrates nervous system starts to form fairly early in embryonic development, after the gastrulation stage, in a process referred to as neurulation, from which the neural tube rises.

The neural tube is initially a monostratified epithelium with its apical side forming the lumenal surface of the tube. As development proceeds neuroepithelial cells divide vigorously in an unsynchronized manner, increasing dramatically its cellular density and acquiring a highly packed, pseudostratified disposition characterized by the presence of cells nuclei at different levels depending on the cell cycle stage they are (reviewd in *Latasa, 2008*).

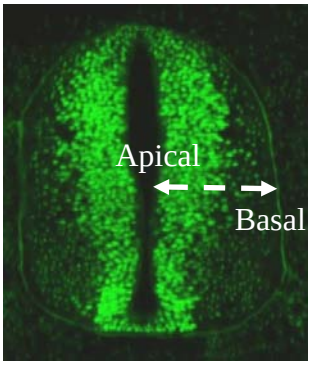

Figure 1. Sox2 stained (transcription factor) (right) **cut view from the neural tube** (image adapted from *www.betacell.org*).

Cells nuclei in the subventricular zone are disposed at different levels along the apical-basal axis according to the cell cycle stage they are. This curious characteristic of the neuroepithelial cells suggests an apical-basal displacement of the nucleus during the cell cycle, a process termed interkinetic nuclear migration (INM).

This nuclear movement spans the entire apical-basal axis of the cell, with the nucleus migrating to the basal side during the first gap (G1) phase of the cell cycle, staying at the basal side during the DNA synthesis phase (S-phase), migrating back to the apical side during the second gap (G2) phase, and undergoing mitosis (M) at the apical side. It is so conserved throughout evolution that it can also be observed in some invertebrates (**Figure 2.**).

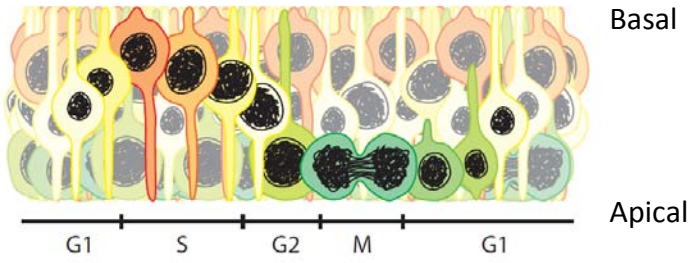

Figure 2. Scheme of the interkinetic nuclear migration observed in vertebrate neuroepithelia. Neuroepithelial cells displace their nuclei as they progress through the cell cycle. During G1, nuclei are displaced to the basal surface, where they undergo DNA replication (S-phase). Once S-phase is finished, nuclei move back to the apical portion of the neuroepithelium as they go through G2, and then they divide to give rise to two daughter cells (M) (*Latasa, 2008*).

Notch signals link the fate decisions of one cell to those of its neighbors and have been shown to be involved in neuronal progenitor maintenance, to govern the decision between the neuronal and glial lineages and to influence aspects of the behavior of terminally differentiated neurons (elaboration of neurites in postmitotic neurons) (reviewed in *Louvi and Artavanis-Tsakonas, 2006*). These signals in this context are not instructive but permissive and are responsible for maintaining a precursor cell in a pluripotent state until the correct differentiation cue is available.

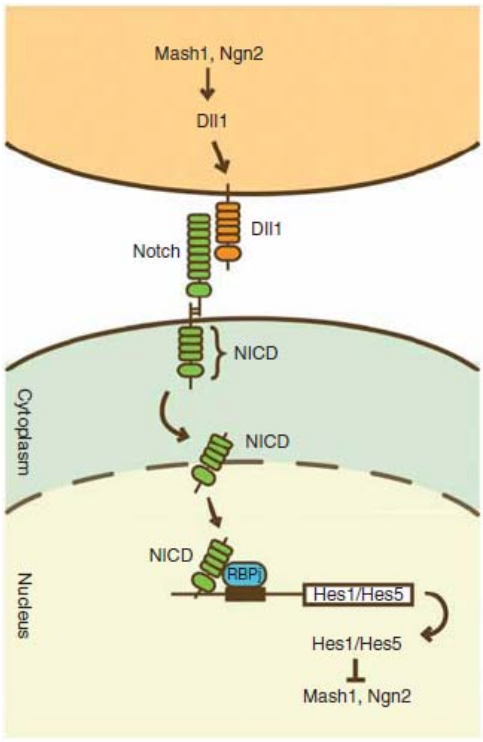

Figure 3. Schematic view of the Notch signaling pathway. The proneural genes *Mash1* and *Ngn2* induce expression of Notch ligands such as Dll1, which activate Notch signaling in neighboring cells. Upon activation, the NICD is released from the transmembrane region and transferred to the nucleus, where it forms a complex with RBPjκ and induces *Hes1* and *Hes5* expression. Hes1 and Hes5 repress proneural gene expression (*Kageyama, 2008*).

Notch pathway, cell cycle INM and neurogenesis

Lateral inhibition is an essential action mechanism by which proneural genes inhibit their own expression in adjacent cells, restricting their own activity to single progenitor cells. This is done by stabilization or amplification of differences between neighbors caused by stochastic events (reviewed in *Artavanis-Tsakonas et al., 1999*).

Moreover, the expression levels of neurogenic and proneural genes have been shown to oscillate as the neural precursors proceed through the cell cycle. During vertebrate development, Notch1 expression increases at the neuroepithelium apical region, where neural precursors going through M are located and the newly generated neurons are born. Also, Dll1 begins to be expressed by the newly born neurons as they initiate their migration through the apical aspect of the neuroepithelium. In this manner, neural precursors basally located within the neuroepithelium, where cells in S-phase are found, show low levels of Notch1, Delta1, Ngn1 and Ngn2, while expression of these genes in proliferating precursors undergoing G2/M/early G1 phases, and situated close to the apical surface, is higher (*Murciano et al., 2002*).

Defining PFGE conditions

Defining new parameters for PFGE requires several trials, adjusting the parameters to obtain the best separation in each of them until the intended result is achieved . However, some empirical calculations may also be performed to restrict the parameters to be used (**Equation 1.**).

$$\max\_resolved\_size\_(kbp) = 0{,}034 \times (T + 40) \times V^{1,1} \times (3 - A)^{0,6} \times t^{0,875}$$

$$\min\_resolved\_size\_(kbp) = 0{,}75 \times \max\_resolved\_size\_(kbp)$$

Equation 1. Relation between the maximum and minimum resolved DNA sizes and the chosen parameters in PFGE. *T* is the chamber's temperature (ºC), *V* is the applied voltage gradient (V/cm), *A* is the agar percentage in the gel (%) and *t* is the pulse time (sec.) pretended (*Current Protocols in Molecular Biology*).

Using the usual values (*T*=14ºC, *V*=6 V/cm and *A*=1% – concentration of the gel) we can calculate the final pulse time needed to establish the maximum resolution size. Because the minimum resolved size is related to the maximum resolved size (**Equation 2.**) and we want to separate fragments up to approximately 256 kbp the choice for the final pulse time has to be centered on that value:

$t = 20\,\text{sec.}:$	$t = 21\,\text{sec.}:$
$\max = 274{,}7 kbp$	$\max = 287{,}7 kbp$
$\min = 206{,}0 kbp$	$\min = 215{,}0 kbp$

Both *t*=20 sec. and *t*=21 sec. could be chosen to delineate the "maximum resolution zone[1]". These values are not restrictive, i.e. using other values one can also separate the same DNA sizes, because different combinations of the parameters can lead to similar results.

Another very important factor that weights in our final pulse time choice is the run time. The longer the run time the better the resolution (thinner bands) however that would cause the smaller DNA fragments to exit the gel, therefore, we have to attend to their migration velocity (**Equation 2.**).

$$10kbp\_velocity(cm/h) = \frac{0{,}0012 \times (T + 25) \times V^{1,6} \times \cos\left(\frac{\theta}{2}\right)}{A}$$

Equation 2. Relation between the 10 kbp sized DNA and the chosen parameters in PFGE. (*Current Protocols in Molecular Biology*).

In our case (*T*=14ºC, *V*=6 V/cm, *θ*=120º and *A*=1%) the 10 kbp sized DNA's velocity would be around 0,411 cm/h. Knowing that the gel is 12 cm length we can only choose run times lower than 29,2 hours (even less because we intend to see DNA sizes even smaller than 10 kbp).

[1] For some authors the maximum resolution zone is limited by the two calculated values and the other zone is called the non-linear migration zone. In our case we considered those two zones as only one, taking it only in account to center on the pretended DNA size.

Table I. PFGE running conditions established after the study.

Parameters	Values
Gel	1%
Initial pulse time	1 sec.
Final pulse time	20 sec.
Run time	20 hours
Voltage	6 V/cm
Angle	120º

The final pulse time chosen was the lowest so that the time increment per hour was the lowest too and the resolution was improved (DNA migrates longer in the same reorientation time which thins the observed bands, as said before). The run time was chosen based on several trials and the old conditions. With the 16 hours runs the smallest bands already migrated down to bottom of the gel and increasing the time up to 20 hours showed to be good for our resolution intents and the smaller bands still appear in the gel.

Comparing "PSI Ψ Clone Big BAC – DNA isolation kit" and Nicoletta's protocol extraction samples

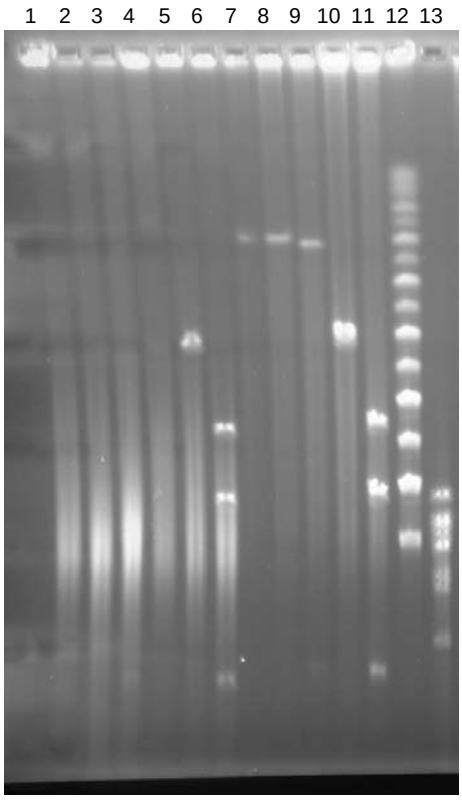

Lanes:

1. **Dll1 BAC Non-digested sample (kit)**
2. **Dll1 BAC AscI digested sample (kit)**
3. **Dll1 BAC NotI digested sample (kit)**
4. **Hes5 BAC Non-digested sample (kit)**
5. **Hes5 BAC AscI digested sample (kit)**
6. **Hes5 BAC NotI digested sample (kit)**
7. **Dll1 BAC Non-digested sample (Nicoletta)**
8. **Dll1 BAC AscI digested sample (Nicoletta)**
9. **Dll1 BAC NotI digested sample (Nicoletta)**
10. **Hes5 BAC AscI digested sample (Nicoletta)**
11. **Hes5 BAC NotI digested sample (Nicoletta)**
12. **Ladder: MidRange II PFG Marker**
13. **Ladder: λ-monocut mix**

Figure 4. MidRange II PFG marker fragments' sizes (left)**, λ-DNA Mono cut mix fragments' sizes** (middle)**, and PFGE photo** (right). All DNA samples obtained using Nicoletta's protocol are visible. Using the kit we can only see the Hes5 BAC bands, with a visible smear though. The samples from the protocol described by Nicoletta show much less smear.

As observed in **Figure 4.**, the extraction protocol described by Nicoletta et al. not only is capable of extracting the BAC but also the purity achieved is much higher than when using the kit. We could say that using the kit we can only extract lower weight DNA constructs (about 150 kbp – *Hes5* BAC size).

It is also deducible that the purification step using the column was the one responsible for degrading the BAC. Moreover, the fact that the temperature does not remain constant during the usage of the kit may also contribute for the degradation of the DNA.

Final extraction protocol

The protocol established in the lab in the end of the study is described below:

This method is suitable for preparing 2 Identical Maxi-Preps DNA amounts.

Inoculate 400 mL LB media supplemented the resistance drug using 500 µL of starter culture (pre-inoculum) and grow overnight (16-24 hrs) at 250 rpm and 32ºC.

Transfer culture into 8 x 50 mL Falcons and centrifuge at 4000 rpm for 10 min. at 4ºC.

Discard supernatant and resuspend each pellet in 8 mL of P1[2] + RNase solution using a 10 mL pipette.

Add 8 mL of freshly prepared P2 solution to each tube, gently invert tube up and several times to mix the contents and leave at room temperature for no longer than 5 min.

To each tube individually: add 8 mL of P3 solution and gently but immediately rock the tube back and forth several times until all P2 turns white. Place the tubes on ice for 1 hour.

Centrifuge at 4000 rpm for 15 min. at 4ºC.

Transfer each supernatant to a new Falcon tube passing it through a double sheet of autoclaved muslin being very careful because the white pellet may become dislodge and fall.

Centrifuge again at 4000 rpm for 15 min. at 4ºC.

Transfer flow through/supernatant (avoid transferring any white precipitate material) to a Falcon tube and add an equal volume (approximately 24 mL) ice-cold isopropanol and mix by inverting tube a few times, leave at room temperature for 5 min.

Centrifuge at 4000 rpm for 15 min. at 4ºC.

Remove supernatant and pulse spin at 4000 rpm.

Remove any remaining isopropanol with a tip and add 0,25 mL TE (Tris/EDTA) to each tube to resuspend the pellet (let remain 10 min. at room temperature).

Using 200 µL cut tips pool the dissolved DNA into 4 x 1.5 mL tubes.

Add 500 µL of phenol:chloroform pH=7,9 to each tube and carefully invert tube 8 times.

Spin 5 min. at 13000 rpm.

Remove each supernatant (top phase) to a new 1,5 mL tube using 200 µL cut tips and repeat Phenol/Chloroform step on it.

Spin 5 min. at 13000 rpm.

[2] The solutions used to perform the established protocol were from *Genopure Plasmid Maxi Kit* by *Roche Applied Science*.

Remove all supernatants (top phase) to 1 new 2ml tube using 200 µL cut tip to pull the DNA and divide the DNA equally between 4 x 1.5 ml tubes.

Add 1 mL ice-cold 100% Ethanol and mix by inverting the tube 4 times.

At this stage 2 tubes should be stored in 100% Ethanol as a backup stock.

Spin 2 tubes 10 min. 13000 rpm.

Remove the supernatant and add 1 mL room temperature 70% Ethanol to each tube mix by inverting tube 4 times to wash the DNA pellets.

Spin 5 min. 13000 rpm.

Carefully remove as much of the supernatant as possible because the pellets might become dislodged from the tube. Thus it is better to aspirate off the supernatant rather than pour it off.

Air dry pellets at room temperature and when the very edge of the pellets turn from white to translucent (most of the Ethanol has evaporated) resuspend each in 100 µL *MilliQ* water. At this step, do not use narrow bore pipette tips to mechanically resuspend the BAC DNA. Instead, allow the *MilliQ* water to sit in the tube with occasional tapping of the bottom of the tube. It should only take 10 min. to dissolve completely at room temperature.

After resuspension the DNA in the 2 tubes can be pooled into 1 tube.

Model validation – Immunocytochemistry for ES cells on cover-slips

Geminin / GFP / DAPI

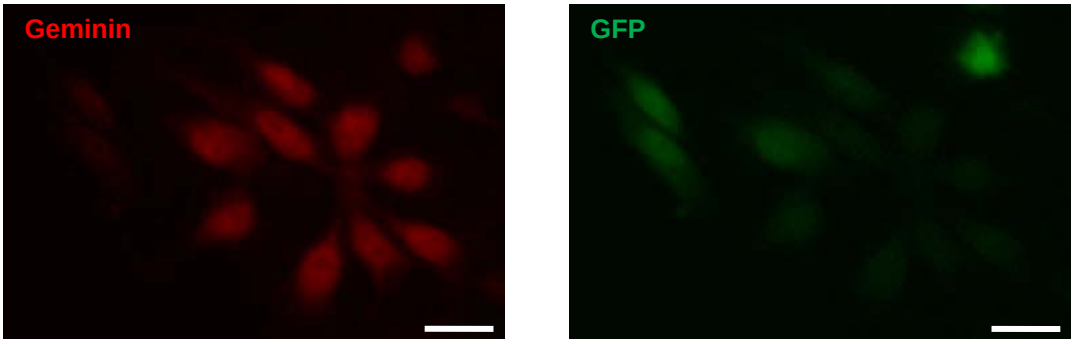

Figure 5. Immunocytochemistry: Geminin/GFP/DAPI (top)**, Geminin** (left) **and GFP** (right)**.** (Bar: 20 µm).

In **Figure 5.** it is observed the nuclei displacement along the rosette according to the cell cycle stage. By assessing the cells stained for Geminin, that recognizes cells in S-phase, G2 and M, we can see that not all cells are recognized and, most important, only cells inside the rosette are stained (cells within the cell cycle).

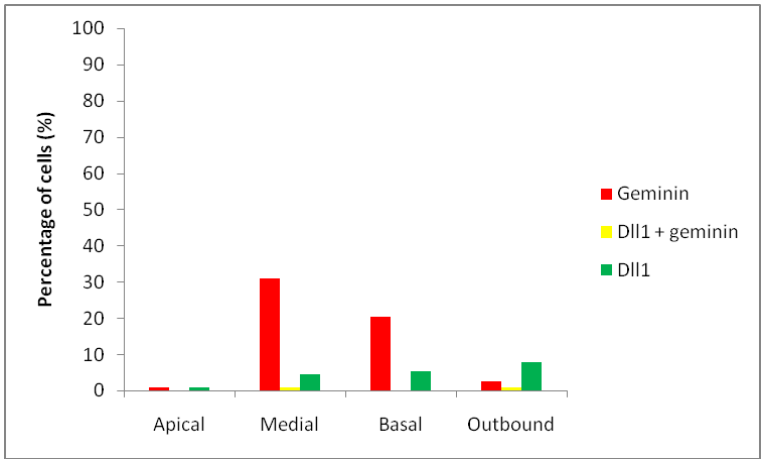

Graphic 1. **Geminin** (red)**, Dll1** (green)**, and Geminin plus Dll1** (yellow) **expression at the rosette's apical-basal axis several levels**. Geminin is expressed mainly in the medial and basal zones of the rosette while Dll1 increases its activity towards the basal side of the rosette.

Regarding **Graphic 1.** we can see that Geminin is mostly expressed in the medial and basal zone of the rosette. These zones have been shown to contain nuclei in G1 and G2 (medial zone), and S-phases (basal layer) of the cell cycle. However, Geminin only stains cells in S-phase, G2 and M, which means that cells only expressing GFP in the medial zone are in G1 or G0 (cell cycle withdrawal). Cells in the apical zone show lower expression of Geminin or GFP. Moreover, no co-localization of the two markers was observed in M (apical zone). However, regarding the percentage of GFP cells in each zone inside the rosette we see that there is a ratio of about 1:4:5 (apical:medial:basal). Mitosis is the shortest phase of the cell cycle (about 5-10% of the cell cycle time only) and, if we look at the values, that is approximately the percentage of the total GFP cells that are found in the apical zone. This means that Dll1 might start being expressed in G2 (co-localization of Geminin and GFP in the medial zone), continue through M, G1 and G0 or through M directly to G0. These results do not contradict this hypothesis already postulated for Dll1 expression in the neural tube which means that the model might be mimicking the Dll1 expression in the neural tube.

As we can see by **Figure 5.**, the several layers from the neural tube are very difficult to limit in the rosettes obtained due the reduced number of cells. However, nuclei observation could also help us characterizing the cells cycle stage and consequently consider the image basing in knowledge introduced in the beginning of this thesis (S-phase and G2 nuclei are bigger than G1 while M nuclei are more dense and very characteristic). Though, even nuclei observation should not be relied in this case.

In the medial and basal layers of the rosette the expression of GFP is almost the same. This agrees with the fact that once a cell expresses Dll1 strongly (commitment to neuronal fate) it does not reenter the cell cycle, and migrates to the outbound of the rosette. The outbound of the neural tube (mantle layer) is where committed neurons accumulate and maturate before migrating. Regarding our data we can see that GFP levels are higher outside the rosettes, as expected too.

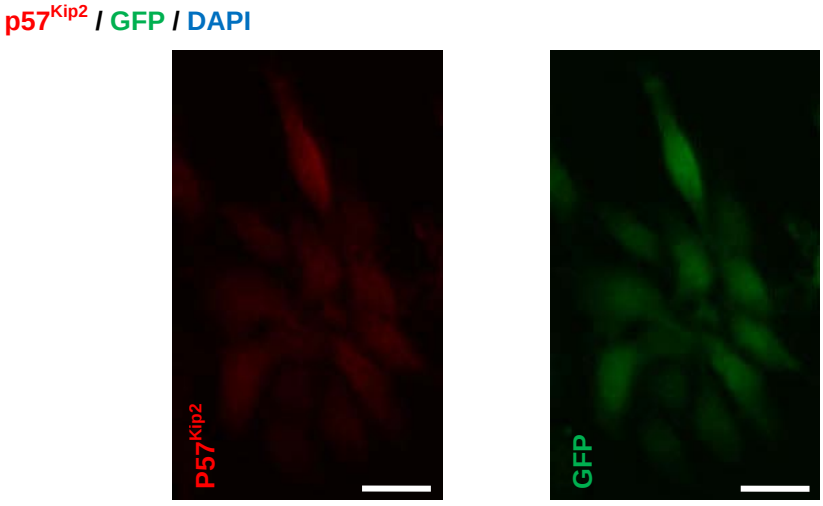

Figure 6. Immunocytochemistry: P57^{Kip2}/GFP/DAPI (top)**, P57^{Kip2}** (left) **and GFP** (right)**.** All cells expressing P57^{Kip2} also express Dll1. (Bar: 20 µm).

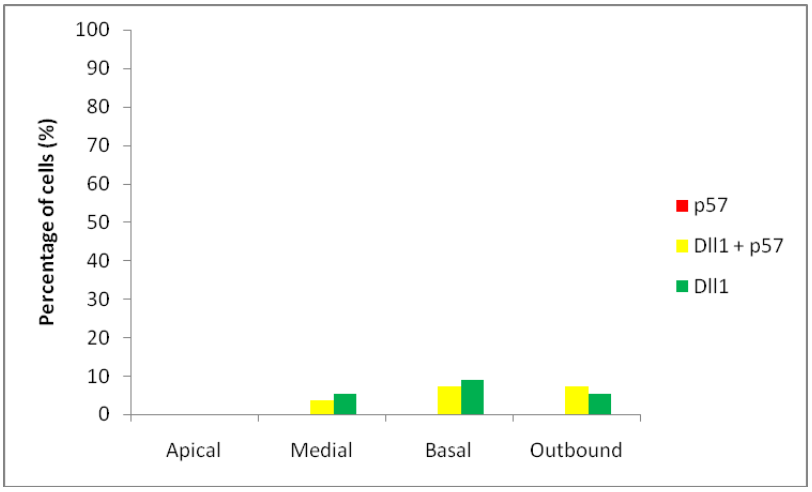

Graphic 2. P57^{Kip2} (red)**, Dll1** (green)**, and P57^{Kip2} plus Dll1** (yellow) **expression at the rosette's apical-basal axis several levels**. P57^{Kip2} is expressed only in cells expressing Dll1. Inside the rosettes, as the levels of P57^{Kip2} increase the expression of both P57^{Kip2} and Dll1 increases too. Outside the rosettes, the majority of cells express both markers and not only Dll1.

Regarding **Graphic 2.** The most striking result is that no cell in the rosettes starts to express p57 ^{Kip2} without expressing GFP, which means that upon cell cycle exit the cells express Dll1 and p57^{Kip2} simultaneously or Dll1 was already being expressed before.

The expression of P57^{Kip2} and GFP in the neural tube is according to expected. The marker p57^{Kip2} is only expressed upon cell cycle withdrawal and during the first neuronal differentiation term, which explains why cells expressing this marker are only found in the medial and basal layers or in the outbound, outside the rosette. Cell cycle exit may happen after M or during G1, but in both cases this would happen in the medial zone predominantly. Therefore, the model is expressing p57^{Kip2} marker in the same way as the neural tube cells.

The cells expressing GFP are also distributed along the cells as expected and as depicted in **Graphic 1.**, i.e. cells in M are not visible, due to reasons stated before, and along

the rest of the rosette the number of cells expressing GFP is similar (there are no evident oscillations occurring in the cells count).

The majority of cells expressing both markers are located in the medial and basal zones or in the outbound of the rosettes, which correlates with the cells cycle exit and the migration stages towards the outside of the rosette, as part of the neuronal differentiation process. We also observe that GFP-single cells in the outbound are as much as the cells expressing $P57^{Kip2}$ and GFP in the same region. This reinforces the fact that $p57^{Kip2}$ is not the only effector of the cell cycle withdrawal mechanism (p21 might be recruited instead).

All Tuj1 and HuC/D cells were shown to also express Dll1. Those two markers only stain cells outside the rosettes (maturing neurons), which confirms the fact that the expression of Dll1 constitutes an important method for monitoring Notch activity, namely concerning neuronal commitment.

However, this data is affected by the low amount of results due to the fact that cells did not grow sufficiently to form dense rosettes as we usually obtain. To have a better and more trustable view and validation of the results one should repeat them and hopefully produce a lot more data to treat.

Conclusion

Although the data obtained for all the assays in the rosettes agrees with the expected behavior if cells were mimicking the neural tube environment, this data is affected by the low amount of results. The cells did not grow sufficiently to form dense rosettes as usually are obtained using the model (as seen in **Figure 12.** of the full version of the thesis). To have a better and more trustable view and validation of the results one should repeat them and hopefully produce a lot more data to treat.

Also, The live imaging of the cells would be an outstanding advance in the study and reliable validation of the model of the rosette structures.

By the global results obtained regarding the model validation we can conclude that the model might be mimicking the neural tube in what concerns the Dll1 ligand expression, because the data did not contradict the several features that have been associated to its expression in the neural tube (accounting on a treatment of the data for the rosettes analogous to the neural tube analysis, i.e. several specific regions according to the cell cycle stage, etc.).

Regarding the results obtained we can say that the model might fit the one proposed by Murciano et al. (**Figure 7.**) to describe the dynamic of the neurogenesis inside the neural tube, with Dll1 being expressed in the called “neurogenic zone” and being in down-regulated in the “pre-neurogenic zone” until the cell gets definitely committed to neuronal fate. This Dll1 oscillations might explain the green “ground-coloring” obtained for cells inside the rosettes,

because the GFP molecules produced inside the cells might not be following the same degradation pattern as the Dll1 molecule.

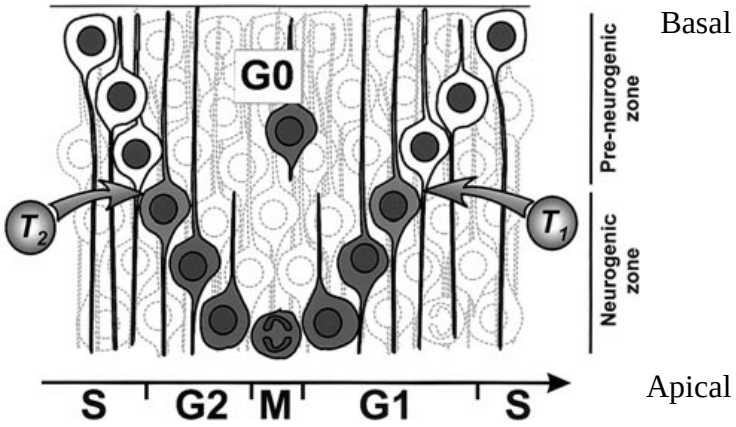

Figure 7. Scheme of the model proposed to represent the functional organization of the neuroepithelium in terms of neurogenesis. The orthogonal arrangement of the cells moving their nuclei up and down as they progress through the cell cycle is translated into the segregation of the neuroepithelium into two zones, each made up of precursors that are transiently involved in distinct functions. In the apical (or ventricular) region (neurogenic zone), proliferating cells are able to express Notch1, Delta1, and the proneural determination gene Ngn2 (dark gray), thus being subjected to lateral inhibition. In the basal epithelium (pre-neurogenic zone), precursors either cannot express these genes or express them at low levels. Postmitotic neurons in G0 still expressing Delta1, Ngn1, and Ngn2 pass through the pre-neurogenic zone as they migrate out from the neuroepithelium. T1 and T2 represent the time points corresponding to the moment in G1 at which the cells lose their neurogenic capacity and the beginning of G2, respectively (image adapted from *Murciano et al, 2002*).

By gathering the data obtained for the assays with $p57^{Kip2}$ and Geminin one can say that cells start expressing Dll1 (neural commitment signalization) before exiting the cell cycle. Co-localization between Geminin and GFP indicates that Dll1 might be expressed even before M. Moreover, it is known that the neural tube has several domains along the anterior-posterior axis and some of them show different expression patterns for several markers. One example is the set of molecules: $p57^{Kip2}$, p21 and Dll1; that show different combinations of expression patterns according to the domain. It has been questioned whether the rosettes model could mimic that capacity to express different patterns according to determined regions and this work could provide the answer for that. Although the observation of static cultured rosettes did not revealed the answer, the dynamic study, once again, would be the most reliable way to assess it.

Restricting the neurogenic capacity to a window prior to cell-cycle exit (G0) probably prevents the execution of the differentiation program during cell-cycle phases prior to M. This prevention mechanism might be happening. As referred before, there was co-localization between Geminin and GFP, though it is still a mystery.

References

Abranches, E., Silva, M., Pradier, L., Schulz, H., Hummel, O., Henrique, D., Bekman, E. (2009). *Neural Differentiation of Embryonic Stem Cells In Vitro: A Road Map to Neurogenesis in the Embryo*. PLoS ONE, Volume 4, Issue 7, 1-14.

BioRad, *CHEF-DR® III Pulsed Field Electrophoresis Systems Instruction Manual and Applications Guide.*

Copeland, N., Jenkins, N., Court, D. (2001). *Recombineering: A POWERFUL NEW TOOL FOR MOUSE FUNCTIONAL GENOMICS*. Nature, Volume 2, 769-779.

C. Wilcock, A., R. Swedlow, J., G. Storey, K. (2007). *Mitotic spindle orientation distinguishes stem cell and terminal modes of neuron production in the early spinal cord.* Development 134, 1943-1954.

Del Bene, F., M. Wehman, A., A. Link, B., Baier, H. (2008). *Regulation of Neurogenesis by Interkinetic Nuclear Migration through an Apical-Basal Notch Gradient.* Cell 134, 1055–1065.

Fior, R., Henrique, D. (2005). *A novel hes5/hes6 circuitry of negative regulation controls Notch activity during neurogenesis*. Developmental biology 281, 318-333.

Fischer, A., Gessler, M. (2007). *Delta–Notch—and then? Protein interactions and proposed modes of repression by Hes and Hey bHLH factors*. Nucleic Acids Research, Volume 35, No. 14.

J. Tomishima, M., Hadjantonakis, A., Gong, S., Studer, L. (2006). *Production of Green Fluorescent Protein Transgenic Embryonic Stem Cells Using the GENSAT Bacterial Artificial Chromosome Library.* Stem cells.

Kageyama, R., Ohtsuka, T., Shimojo, H., Imayoshi, I. (2008). *Dynamic Notch signaling in neural progenitor cells and a revised view of lateral inhibition*. Nature, Volume 11, 1247-1351.

Kessaris, N., Richardson, B. (2006). *DNA Isolation from PAC or BAC Clones*.

Kopan, R., Ilagan, M. (2009). *The Canonical Notch Signaling Pathway: Unfolding the Activation Mechanism*. Cell 137, 216-233.

Latasa, M., Cisneros, E., Frade, J. (2008). *Interkinetic nuclear migration and the coordination between cell cycle and neurogenesis in the vertebrate central nervous system*.

L. Frank, C., Tsai, L. (2009) *Alternative Functions of Core Cell Cycle Regulators in Neuronal Migration, Neuronal Maturation, and Synaptic Plasticity*. Neuron review 62.

Louvi, A., Spyros Artavanis-Tsakonas, S. (2006). *Notch signaling in vertebrate neural development*. Nature, Volume 7, 93-102.

Murciano, A., Zamora, J., López-Sánchez, J., Frade, J. (2002). *Interkinetic Nuclear Movement May Provide Spatial Clues to the Regulation of Neurogenesis*. Molecular and Cellular Neuroscience 21, 285-300.

Nature, *Neurosciences reviews*.

Rodrigues.C. (2007). *Novel Strategies For Gene Manipulation in Mammalian Cells*. Dissertação para obtenção do Grau de Mestre em Engenharia Biológica.

Shimojo, H., Ohtsuka, T., Kageyama, R. (2008). *Oscillations in Notch Signaling Regulate Maintenance of Neural Progenitors.* Neuron 58, 52–64.

Silva, J., Smith, A. (2008). *Capturing Pluripotency.* Cell 132(4): 532-536.

Smith, A. (2001). *EMBRYO-DERIVED STEM CELLS: Of Mice and Men*. Annu. Rev. Cell Developmental Biology, 17:435-62

Wiley, J. and Sons (2007). *Current Protocols in Molecular Biology.* Current protocols.

Ying, Q., G. Smith, A. (2003). *Defined Conditions for Neural Commitment and Differentiation.* Methods in enzymology, VOL. 365

Ying, Q., Nichols, J., Chambers, I., Smith, A. (2003). *BMP Induction of Id Proteins Suppresses Differentiation and Sustains Embryonic Stem Cell Self-Renewal in Collaboration with STAT3*. Cell, Volume 115, 281-292.

Ying, Q., Stavridis, M., Griffiths, D., Li, M., Smith, A. (2003). *Conversion of embryonic stem cells into neuroectodermalprecursors in adherent monoculture*. Nature.

Ying, Q., Wray, J., Nichols, J., Batlle-Morera, L., Doble, B., Woodgett, J., Cohen, P., Smith, A. (2008). *The ground state of embryonic stem cell self-renewal.* Nature, Volume 453.